Renewable Energy 36 (2011) 1437–1446

Contents lists available at ScienceDirect

Renewable Energy

journal homepage: www.elsevier.com/locate/renene

Local wind-energy potential for the city of Guelph, Ontario (Canada)

Joseph H. McIntyre [a], William D. Lubitz [a,*], Warren H. Stiver [a,b]

[a] School of Engineering, University of Guelph, Guelph, ON N1G 2W1, Canada
[b] NSERC Chair in Environmental Design Engineering, Canada

ARTICLE INFO

Article history:
Received 20 March 2010
Accepted 23 October 2010
Available online 24 November 2010

Keywords:
Urban wind energy
Resource assessment
Turbine power curve
Data modeling

ABSTRACT

Municipalities around the world are using community energy plans (CEPs) to drive progress towards a more sustainable energy future. Many recognize the supply of local and renewable energy as a crucial component of a resilient future including the potential use of wind power generation. The city of Guelph (Ontario, Canada) included wind energy as a component of its CEP. The goal of this work was to estimate the potential for wind power generation within the municipal boundaries of this city. This paper summarizes the methodology used and results obtained with site and meteorological data, wind maps, and turbine power curves. The methodology relies on the use of a geographically uniform array of turbines, spread throughout the community. An array of utility-scale turbines could potentially generate 29% of Guelph's 2005 total electricity demand, whereas one consisting of small-scale turbines could achieve 10% of that demand.

1. Introduction

Community energy planning is a relatively new and growing part of urban planning activities. A growing number of municipalities are developing and implementing these plans (CEPs) for long-term energy availability with respect to location, population, and commerce [1]. Several guides exist for the evaluation, creation, and implementation of such plans [2–4]. The Canadian Urban Institute demonstrated leadership and commitment to this process by developing and providing tools that examine the spatial dimensions of municipal energy supply and demand [5]. The final CEP stands as a target towards which communities work to ensure that future energy supply and demand remain in-sync and allow for the continuance of their quality-of-life aspirations. For many, these plans embrace sustainability with respect to energy and in considerations of economic, environmental, and social contexts while allowing for prioritization and balance of these issues. Additionally, some utilize CEPs to incorporate local energy generation with demand reduction strategies (including changes to the built environment) to minimize environmental impact while increasing energy security [6]. A survey of ten Canadian CEPs found that the primary motivators for their development were energy conservation and the reduction of greenhouse gas emissions [1].

Potential exists for the development of wind power generation within cities. Although rare, the placement of wind turbines within urban communities does occur [7]. Furthermore, community ownership of conventional wind-power projects, sometimes located in close proximity to towns, is well established in Europe [8] and becoming more common in North America [9]. The use of conventional energy resources currently costs less than the incorporation of technology to utilize distributed renewable resources [10]. That said, long-term uncertainty related to the supply and cost of non-renewable resources makes it impractical to exclude the use renewable resources from CEPs.

Several methods exist for the evaluation of wind resources over a specified region including the use of computational fluid dynamics (CFD) [11] or boundary layer wind tunnels [12]. Major wind-resource assessment tools such as WAsP and WEST/Anemograph utilize meteorological station data to infer geostrophic-height winds and approximate local conditions at heights of interest [13,14]. These approaches however are resource and time intensive, and it is fortunate that wind maps are now common and generally available for most regions of the world. As a component of this study, we explored how accurately regional wind resources could be approximated using wind map and weather station data, while avoiding more onerous modeling processes.

The city of Guelph covers 86.72 km^2 of land and, as shown in Fig. 1, lies approximately 100 km west, southwest of Toronto in Ontario (Canada). Guelph had a population of ca 115 000 in 2006 [15], and planners anticipate that figure to reach 150 000 by 2021

Abbreviations: CEP, community energy plan; ERS, Elora Research Station; EVLF, Eastview Landfill; GTI, Guelph Turfgrass Institute; CWEA, Canadian Wind Energy Atlas; OWRA, [Ontario] Wind Resource Atlas; J&M, Justus and Mikhail model; PL, power law model; MMLM, modified maximum likelihood method; WPD, Weibull probability distribution.

* Corresponding author. Tel.: +1 519 824 4120x54387; fax: +1 519 836 0227.
E-mail address: wlubitz@uoguelph.ca (W.D. Lubitz).

0960-1481/$ – see front matter © 2010 Elsevier Ltd. All rights reserved.
doi:10.1016/j.renene.2010.10.020

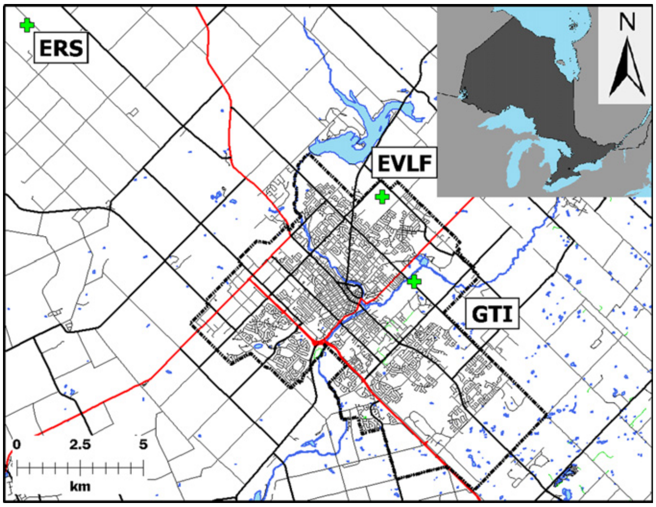

Fig. 1. Map of city of Guelph with location of the two weather stations and EVLF.

based on a medium-growth scenario [16]. Guelph approved its CEP in 2007 [17] and recently began the process of its implementation. The CEP called for a reduction in energy demand within 25 years while shifting to renewable resources. Furthermore, the plan acknowledged that wind could help the city attain its energy goals. However, an important and hitherto unanswered question remained: how much wind energy could potentially be harnessed within the city of Guelph?

The primary objective of this work was the development of a first estimate of an upper-limit, wind-energy potential within the city limits of Guelph. The evaluation of the wind resource relied on local meteorological and site wind data as well as publicly available atlases. We utilized an evenly-dispersed grid for the acquisition of discrete data from the wind atlases. The subsequent wind-energy potential estimates involved the application of the resource results to two commercially-available turbine power curves with scaling to uniformly-distributed, idealized arrays that blanketed the city. Throughout this paper, the term 'grid' refers to the locations utilized for wind atlas data acquisition, whereas 'array' implies the scaling of the wind-energy results to estimate the city's total potential. This first estimate is a hypothetical value in that the uniformly-dispersed array ignores geographic, structural, and legal constraints that preclude the placement of turbines. Following the estimate, we compared the results of this estimate with the city's total energy and electricity demand for the year 2005. We presented a first iteration of this work at the World Wind Energy Conference, 2008 (Kingston, Ontario; Canada) [18].

2. Methods and materials

Fig. 2 shows the sequence of application for the methods and models used in this study to estimate of wind-energy potential in Guelph. The combination of different data sources (e.g. site, meteorological station, or wind atlas) and methods allowed for a comparison of the different approaches utilized. This section describes each component of the analysis.

2.1. Meteorological station data

The Agrometeorology group of the Department of Land Resource Science at the University of Guelph operates weather stations at the Guelph Turfgrass Institute (GTI) and at the Elora Research Station (ERS). The GTI lies on the eastern side of the city (43° 32′ 55″ N, 80° 13′ 1″ W; altitude 325 m), and the ERS sits in open agricultural fields approximately 15 km north-northwest of the city (43° 38′ 28″ N, 80° 24′ 20″ W; altitude 376 m) [19]. The facilities, shown in Fig. 1, are maintained according to Environment Canada standards for weather monitoring stations. These stations recorded 1-h average directional and wind-speed data at 10 m above ground.

2.2. Wind energy site assessment data

In 2003, the city of Guelph closed the Eastview Landfill (EVLF; 43° 34′ 43″ N, 80° 13′ 56″ W; altitude 325 m), located in the northeastern corner of the city (see Fig. 1). After its closure, the city commissioned a one-year study of wind-energy potential at EVLF. That study provided 10-min average wind-speed and directional data at 20 and 30 m above ground from December 7th, 2003 to December 12th, 2004, as recorded with NRG anemometers [20]. We excluded data acquired after December 9th, 2004 due to erratic observations that indicted inverted shear and suggested a failure of the measurement system. In this study, we generated and analyzed

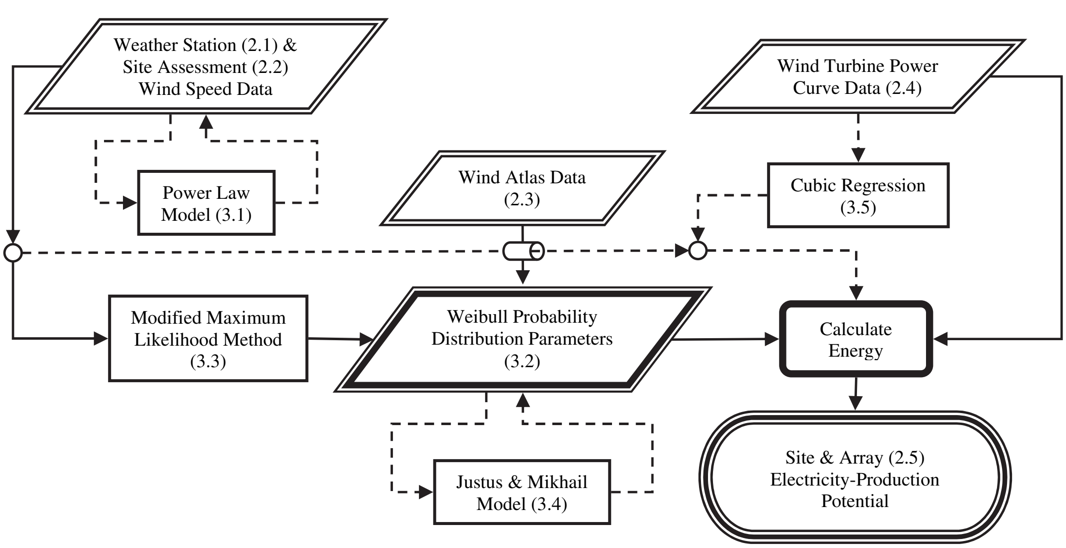

Fig. 2. Process flow diagram describing the application of data, models, and methods utilized in this study.

a 1-h data set by averaging the respective 10-min data. This allowed us to examine the impact of time resolution on the results for the EVLF and compare these results with that from the meteorological stations.

2.3. Wind atlas data

There were two publicly available wind-resource atlases that covered Guelph. Environment Canada sponsors the Canadian Wind Energy Atlas (CWEA) which provided annual and seasonal (3-month increment) data at 30, 50, and 80 m above ground [21]. The CWEA data represented observations made between 1958 and 2000. The Ontario Ministry of Natural Resources offers the [Ontario] Wind Resource Atlas (OWRA) which provided annual data at 30 and 80 m above ground, as derived from observations made between 1984 and 2002 [22]. Both atlases report mean wind speed, WPD parameters, and wind roses for locations in Canada and Ontario, respectively. The spatial resolutions of the CWEA and OWRA were 5 km [21] and 200 m [23], respectively, at the time of data acquisition.

2.4. Wind turbine power curves

This study simulated the use of two representative examples of small- and utility-scale wind turbines. We selected the Excel-S of the Bergey Windpower Company to represent the small-scale unit. The Excel-S has a 7 m rotor diameter, a cut-in speed of 3.6 m/s (8.1 mph), and a manufacturers' rating of 10 kW at 13.9 m/s (31 mph) [24]. We utilized the publicly available power curve provided by the manufacturer with a turbulence factor of 15% and a site altitude of 356 m. We opted for the Vestas V82 to represent an inland megawatt-scale wind turbine and applied the manufacturer's power curve [25]. The V82 has an 82 m rotor diameter, a cut-in speed of 3.5 m/s (7.8 mph), and a manufacturers' rating of 1.65 MW at 13.5 m/s (30 mph). Fig. 3 shows the power-density output curves of these turbines.

2.5. Community-scale power generation

Estimation of the wind-energy potential from city-wide arrays involved two approaches. Each used the number of evenly spaced turbines that could fit within the city limits of Guelph. The evenly spaced turbines meant ignoring the geographical and structural features of the city, as well as any ordinances that may preclude placement [18]. This spacing led to an upper-limit estimate of the wind-energy potential within the city limits, as actual production should be lower as a result of siting constraints. We based the turbine spacing on a square footprint with a characteristic length of 10 rotor diameters. For Guelph, a idealized array of Excel-S turbines consisted of 17 697 units, while the span of a V82 limited that number to 128. The estimates included the output potential for arrays consisting of either Excel-S or V82 turbines at hub heights of 30 and 80 m, respectively. For each array, we applied a 10% penalty to account for downwind wake effects [26].

The first approach was a simple multiplication of the number of turbines that would fit in the community by the electricity production of one turbine at a single site (ERS, GTI, or EVLF). Under this approach, all turbines in the array generated an electrical output equal to that of one located at the specific site.

For the second approach, we captured the spatial variability of the wind resource throughout the community using wind atlas data. This involved the use of a 35-point grid that overlaid the city that we utilized to gather data. The resolution of the CWEA permitted the identification of 10 unique data sets, while the OWRA

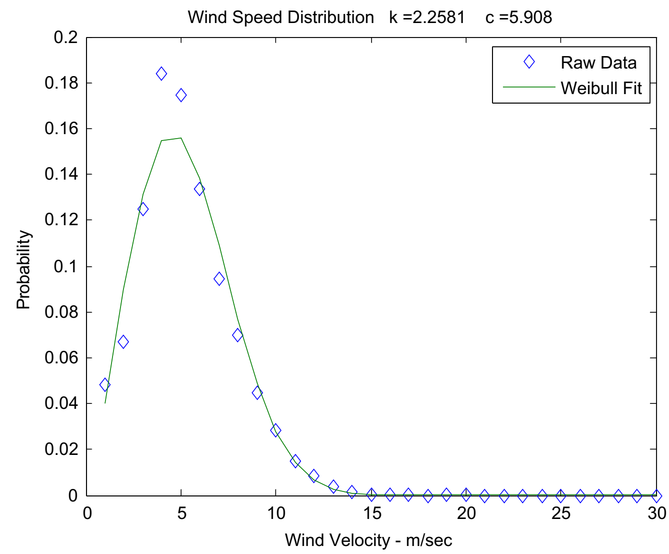

Fig. 4. An example of the output obtained using the MMLM to determine WPD parameters from wind-speed data. {Note: obtained from annual EVLF site data with the original, 10-min observation data at 30 m above ground}.

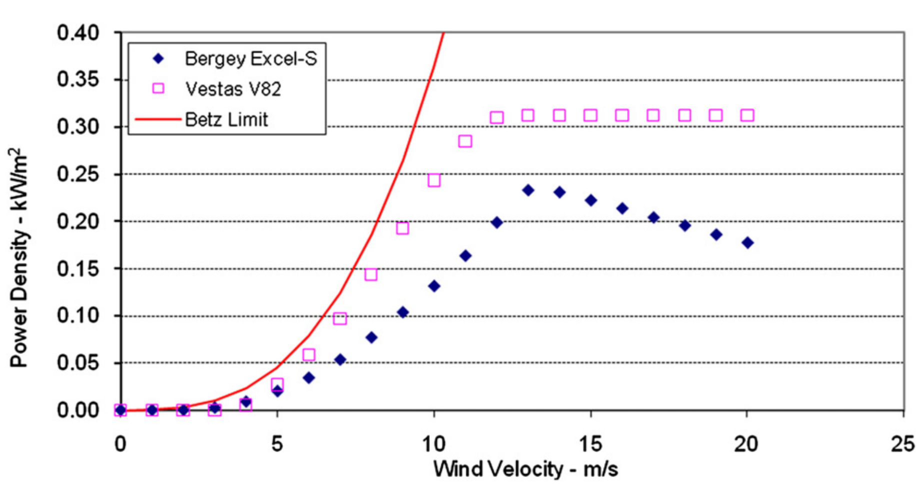

Fig. 3. Power density (output normalized by swept area) versus wind speed for Bergey Excel-S [1] and Vestas V82 [25] wind turbines as compared to the theoretical Betz Limit.

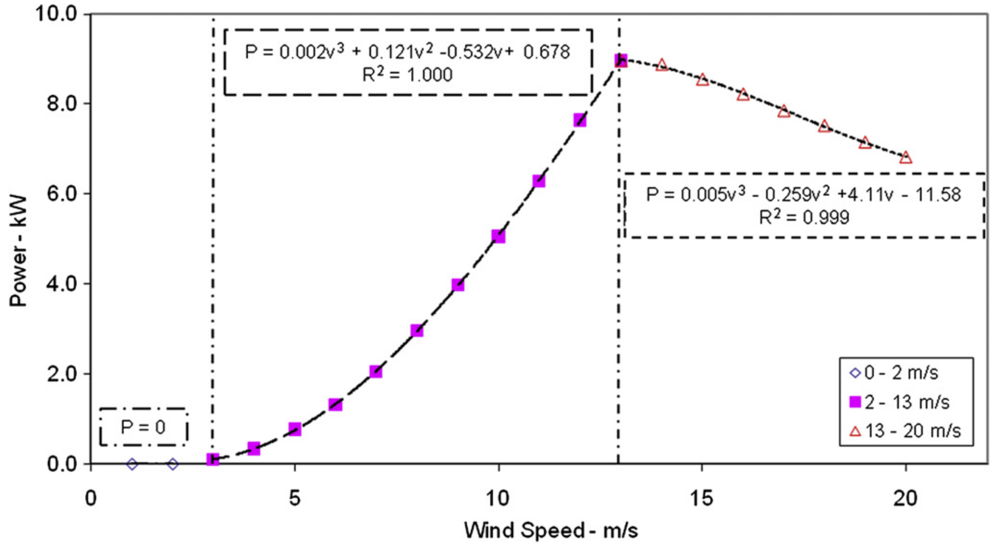

Fig. 5. The three-segment cubic-regression model (CR) of the Bergey Excel-S power curve [1].

provided unique results for each grid point. We scaled the CWEA results according to the replication of data with respect to the thirty-five grid points (i.e. samples); this was unnecessary for the OWRA data. Finally, the estimation of the output potential involved the application of these results to the number of turbines in each array.

3. Theory and calculations

3.1. Power law model

Wind-speed data acquisition for the GTI and ERS occurred at a height of 10 m above ground, while that of the EVLF occurred at 20 and 30 m. Use of the power law model (PL),

$$v(z) = v_a\left(\frac{z}{z_a}\right)^{\alpha}, \tag{1}$$

allowed for the height adjustment of the data to that of the proposed hub heights for the Bergey (30 m) and Vestas (80 m) turbines. Here, v represents the wind speed at height z with the subscript ‘a’ denoting actual observation. Counihan [27] provided the equation

$$\alpha = 0.096\log_{10}(z_0) + 0.016(\log_{10}(z_0))^2 + 0.24, \tag{2}$$

which we applied to calculate the power law exponent, α. Here, z_0 (in m) represents the characteristic roughness length of the terrain in the area of interest. Manwell et al. [26] listed roughness-length values for the PL according to the type of terrain. Using this reference, we selected roughness lengths of 1.5 m for the GTI and EVLF, and 0.10 m for the ERS, which resulted in coefficient values of 0.26 and 0.16, respectively. The recording of observation data at two heights for the EVLF allowed for the derivation of a second coefficient value by utilizing Eq. (1). Our subsequent referral of power coefficients associated with the PL reflects the value of α. Subsequent referral to the PL coefficient as ‘assumed’ reflects the selection and use of a roughness length in Eq. (2), whereas ‘calculated’ indicates that α was inferred from multiple-height data.

3.2. Weibull probability distribution

Predicting wind turbine power output requires knowledge of the distribution of expected wind speeds. The Weibull continuous probability distribution model [28] is the most commonly used model for the assessment of wind-speed variation [29]. Numerous studies indicate that this model accurately characterizes time-

Table 1
Annual single-turbine production potential at 30 m above ground as calculated using WPD parameters obtained from 1-h site data (GTI and ERS, raw; EVLF, time-averaged) and modeled using the Bergey Excel-S power curve.

Site	Time span	Observation height (m)	Wind speed (m/s)		Power coefficient	WPD parameters		Potential output (MWh)	Model
			Mean	Std. dev.		k	c (m/s)		
GTI	94–04[a]	10	N/A	N/A	0.255	1.99	4.89	7.56	J&M
GTI	94–04[a]	10	4.27	2.65	0.257[b]	1.74	4.86	8.39	PL
GTI	03–04[a]	10	N/A	N/A	0.251	2.07	5.09	8.23	J&M
GTI	03–04[a]	10	4.45	2.69	0.257[b]	1.79	5.08	9.18	PL
ERS	94–04[a]	10	N/A	N/A	0.238	1.95	5.83	12.3	J&M
ERS	94–04[a]	10	4.74	2.83	0.160[b]	1.76	5.34	10.6	PL
ERS	03–04[a]	10	N/A	N/A	0.236	1.93	5.91	12.8	J&M
ERS	03–04[a]	10	4.83	2.93	0.160[b]	1.73	5.44	11.2	PL
EVLF	03–04[a]	30	5.22	2.40	N/A	2.32	5.90	11.5	MMLM
EVLF	03–04[a]	20	N/A	N/A	0.238	2.28	5.81	11.1	J&M
EVLF	03–04[a]	20	5.17	2.52	0.257[b]	2.18	5.85	11.6	PL
EVLF	03–04[a]	20	5.13	2.50	0.241[c]	2.18	5.80	11.4	PL

[a] 2003-341, 1300 to 2004-344, 0800.
[b] PL-assumed.
[c] PL-calculated.

Table 2
Annual single-turbine production potential at 30 m above ground as calculated using WPD parameters obtained from 10-minute EVLF site data and modeled using the Bergey Excel-S power curve.

Site	Time span	Observation height (m)	Wind speed (m/s)		Power coefficient	WPD parameters		Potential output (MWh)	Model
			Mean	Std. dev.		k	c (m/s)		
EVLF	03–04[a]	30	5.22	2.46	N/A	2.26	5.91	11.7	MMLM
EVLF	03–04[a]	20	N/A	N/A	0.238	2.22	5.81	11.3	J&M
EVLF	03–04[a]	20	5.17	2.58	0.260[b]	2.13	5.87	11.8	PL
EVLF	03–04[a]	20	5.13	2.56	0.241[c]	2.13	5.81	11.6	PL

[a] 2003-341, 1300 to 2004-344, 0800.
[b] PL-assumed.
[c] PL-calculated.

series, wind-speed data for various situations [30]. The Weibull probability distribution (WPD) model provides the probability, p, of the wind achieving speed, v, as described by the shape and scale factors, k and c, respectively:

$$p(v) = \left(\frac{k}{c}\right)\left(\frac{v}{c}\right)^{k-1}\exp\left[-\left(\frac{v}{c}\right)^{k}\right]. \tag{3}$$

3.3. Modified maximum likelihood method

The modified maximum likelihood method (MMLM) is a proven method for superior accuracy in the estimation of WPD parameters for wind-speed data [31]. The method utilizes two equations: the first requiring an iterative calculation to determine the shape factor, k,

$$k = \left(\frac{\sum_{i=1}^{n} v_i^k \ln(v_i)P(v_i)}{\sum_{i=1}^{n} v_i^k P(v_i)} - \frac{\sum_{i=1}^{n} \ln(v_i)P(v_i)}{P(v_i \geq 0)}\right)^{-1}; \tag{4}$$

followed by a calculation of the scale factor, c:

$$c = \left(\frac{1}{P(v_i \geq 0)}\sum_{i=1}^{n} \ln(v_i)P(v_i)\right)^{1/k}. \tag{5}$$

For these equations, v_i, is the central wind speed for each bin, i; $P(v_i)$ indicates the frequency of occurrence in the bin; and $P(v_i \geq 0)$ represents the probability of the wind speed being greater-than-or-equal-to zero. Execution commenced with an initial k value of 2.0 (a Rayleigh distribution), and continued iteratively until the square of the difference between the new and previous values was less than 10^{-10}. We utilized 30 bins, n, with discrete wind-speed intervals of 1 m/s in the calculations. Note that the International Electrotechnical Commission (IEC) recommends intervals of 0.5 m/s for the generation of wind turbine power curves [32]. Fig. 4 shows an example of a WPD obtained using the MMLM algorithm. The designation PL in the remainder of this paper indicates the application of the PL followed by the MMLM to obtain WPD parameters. The notation MMLM in the resulting tables indicates a height match between the data and the proposed turbine hub and the exclusion of the PL.

3.4. Justus and Mikhail model

Justus and Mikhail [33] provided a model (J&M) that utilizes WPD parameters for wind speed at one height to estimate parameters for another height. The equations for this model are

$$k(z) = k_a\frac{[1-0.0881\ \ln(z_a/10)]}{[1-0.0881\ \ln(z/10)]}, \tag{6}$$

and

$$c(z) = c_a\left(\frac{z}{z_a}\right)^n, \tag{7}$$

with n calculated as

$$n = \frac{[0.37-0.0881\ \ln c_a]}{[1-0.0881\ \ln(z_a/10)]}. \tag{8}$$

Table 3
Data utilized for the various methods of analysis.

Site	Time span	Observation height (m)	Number of data points used			Method of analysis
			Theoretical	Maximum	Minimum	
GTI	94–04	10	96 432	87 542 (90.8%)	87 542 (90.8%)	MMLM, J&M, PL
GTI	03–04[a]	10	8828	3490 (39.5%)	3490 (39.5%)	MMLM, J&M, PL
ERS	94–04	10	96 432	95 301 (98.8%)	95 301 (98.8%)	MMLM, J&M, PL
ERS	03–04[a]	10	8828	8824 (100%)	8824 (100%)	MMLM, J&M, PL
EVLF	03–04[a]	30	52 961	52 961 (100%)	52 961 (100%)	MMLM, J&M, PL
EVLF	03–04[a]	20	52 961	52 961 (100%)	52 961 (100%)	MMLM, J&M, PL
EVLF	03–04[a]	30	8828	8828 (100%)	8828 (100%)	1-h
EVLF	03–04[a]	30	8828	8828 (100%)	8828 (100%)	1-h
EVLF	03–04[a]	20	8828	8828 (100%)	8828 (100%)	1-h
EVLF	03–04[a]	20	8828	8828 (100%)	8828 (100%)	1-h
GTI	94–04	10	96 432	88 421 (91.7%)	88 401 (91.7%)	CR
GTI	03–04[a]	10	8828	3652 (41.4%)	3652 (41.4%)	CR
ERS	94–04	10	96 432	95 447 (99.0%)	95 024 (98.5%)	CR
ERS	03–04[a]	10	8828	8824 (100%)	8822 (99.9%)	CR
EVLF	03–04[a]	30	52 961	52 961 (100%)	52 951 (100%)	CR
EVLF	03–04[a]	30	52 961	52 961 (100%)	52 953 (100%)	CR
EVLF	03–04[a]	20	52 961	52 961 (100%)	52 944 (100%)	CR
EVLF	03–04[a]	20	52 961	52 961 (100%)	52 951 (100%)	CR

[a] 2003-341, 1300 to 2004-344, 0800.

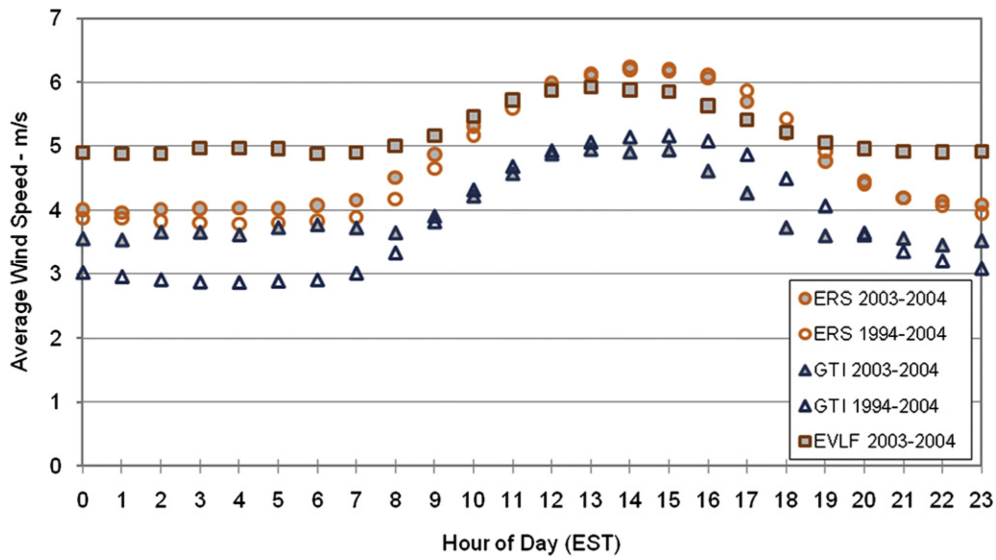

Fig. 6. Diurnal mean wind-speed variation for the ERS, GTI, and EVLF during the evaluated time periods.

The WPD parameters *k* and *c* correspond to a height above the ground, *z*, with the subscript 'a' denoting those obtained with the actual-observation data. Subsequent referral to the power coefficients associated with the J&M relates to the value of *n*. The designation J&M indicates the adjustment of WPD parameters obtained with the MMLM from observation height to the proposed hub height.

3.5. Cubic-regression model of wind turbine power curve

The investigation of the wind-energy output potential in the absence of a WPD required a turbine power curve in the form of a continuous function rather than discrete tabular data. Production of this continuous-function power curve involved the segmentation of the manufacturer's power curve into three portions followed by cubic-regression analysis (CR). Fig. 5 shows the power curve with the equations obtained via regression analysis for the Bergey Excel-S. We estimated the annual potential-energy production by multiplying the total hours in the observation period with the sum of energy produced for each wind-speed measurement. Finally, the production potential required normalization to an annual timeframe to obtain the final results. With the exception of the 30 m observation-height data for the EVLF, we obtained all height-adjusted wind-speed data via the PL. As such, the use of the designation CR in this paper typically indicates the use of the PL prior to estimation of the potential output via this strategy.

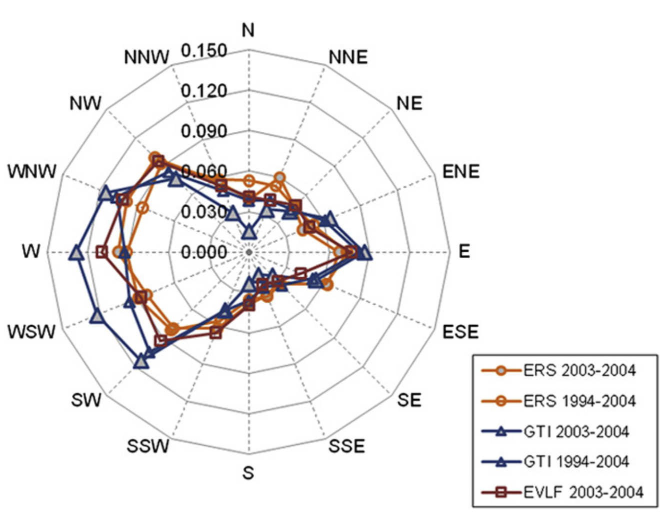

Fig. 7. Wind-direction frequency distribution for the ERS, GTI, and EVLF during the evaluated time periods.

4. Results and discussion

This study involved the application of several methods and models to data from multiple sources in order to estimate the wind-energy potential within the municipal limits of the city of Guelph. Fig. 2 highlights the application sequence of the data and models utilized in this study and described in Sections 2 and 3. The left side of this diagram portrays the use of site assessment and meteorological station data for the three locations for wind-speed observation utilized in this study. The central part of Fig. 2 focuses on the heart of this assessment, the determination of Weibull probability distributions (WPDs) for wind speed. The right of Fig. 2 illustrates the combination of the wind-speed distributions with the power curves to estimate annual and seasonal wind-energy potential within Guelph.

Table 1 presents the single-turbine results obtained with the 1-h data from the ERS, GTI, and EVLF at 30 m above ground. This table includes those from the modified EVLF data, while Table 2 shows that obtained with the original, 10-min EVLF data at this height. The results presented in these tables cover the 1994–2004 and 2003–2004 time spans and involved height adjustment with the PL and J&M. As shown, we used the Bergey Excel-S power curve as the basis of comparison for the bulk of this assessment. Similarly, the PL served as the basis of comparison for the meteorological and site data. During the 2003–2004 period, the EVLF site exhibited the highest wind-speed average while the ERS displayed the greatest variation. The differences in wind-speed average and standard deviation of the ERS indicate that the 2003–2004 period was slightly windier than that of 1994–2004. Review of the GTI data during the 2003–2004 period revealed that 60% of the observations recorded were erratic; most of which occurred between March 1st and October 1st of 2004. This period coincided with seasons previously found to have the lowest wind-energy potential for Guelph [18]. As a result, we anticipated that the estimates of the potential output at the GTI would be lower relative to other values

Table 4
Annual single-turbine production potential at 30 m above ground as calculated by direct application of a three-segment cubic-regression (CR) model of the Bergey Excel-S power curve as applied to the wind-speed data.

Site	Time span	Observation height (m)	Wind speed (m/s)		Power coefficient	Potential output (MWh)	Relative variation (basis)		
			Mean	Std. dev.			MMLM	J&M	PL
GTI	94–04	10	4.23	2.67	0.257[b]	8.27	N/A	9.4%	−1.4%
GTI	03–04[a]	10	4.25	2.78	0.257[b]	8.77	N/A	6.5%	−4.5%
ERS	94–04	10	5.28	3.17	0.160[b]	10.6	N/A	−13.6%	−0.1%
ERS	03–04[a]	10	4.83	2.93	0.160[b]	11.4	N/A	−11.2%	1.2%
EVLF	03–04[a]	30	5.22	2.46	N/A	11.5	*−1.8%*	N/A	N/A
EVLF	03–04[a]	20	5.17	2.58	0.260[b]	11.6	N/A	3.1%	−0.6%
EVLF	03–04[a]	20	5.13	2.56	0.241[c]	11.4	N/A	1.0%	−2.6%

[a] 2003-341, 1300 to 2004-344, 0800; italicized values indicate those determined from unadjusted data; underlined values are relative to average of PL values.
[b] PL-assumed.
[c] PL-calculated.

found for this period. Table 3 provides an assessment of validity for the site and meteorological data used in this study. This includes the number of theoretically-available observations based on the time span and the maximum and minimum utilized along with the method(s). A discrepancy between the maximum and minimum number of datum applied during modeling may occur due to the application of the methods and models. As shown, most or all of the data taken at the EVLF and ERS sites were valid.

The ERS data covered both the 1994–2004 and 2003–2004 timeframes with high proportions of validity. For this reason, we utilized the results obtained with that data as a basis of comparison for the sites within the city of Guelph. The similarity of observations made in this study with those of other sources supported this decision. Fig. 6 displays the diurnal wind-speed cycles found for the ERS, GTI, and EVLF during these periods. As shown, the trends exhibited minimal hourly variation from evening (1900) through to the early morning (700) followed by a symmetrical curve with a maximum occurring between 1300 and 1500 h. This pattern duplicates the observations of Li and Li [34] for the Waterloo Wellington meteorological station (43° 27′ N, 80° 22′ W; altitude 317 m) for the 1999–2003 period. That site lies approximately 10 km southwest of Guelph. Fig. 7 shows the wind-direction frequency at the ERS, GTI, and EVLF for the timeframes evaluated. During those periods the wind proceeded from the west 55–64% of the time. These wind roses generally concur with those provided by the CWEA and OWRA for the respective sites, as well as those found by Li and Li [34]. Note that the wind roses of the OWRA lacked directional designation. The resemblance of the results obtained in this study with those made by Li and Li [34] indicates that these sites share a similar wind regime.

Table 1 and Table 2 include the results obtained with the modified and original EVLF data, respectively. The results obtained with the EVLF data for both time increments were consistent. The potential output based on the modified, 1-h data was between 1.2% and 2.0% less than that of the original, 10-min data. At some point, a magnitude of change in the observation increment and period should alter the shape of the wind-speed distribution and result in marked difference in wind-energy potential. However, this did not occur for the EVLF data at these time resolutions.

The comparison of wind-energy potential at the selected sites began with an assessment of the potential variation in single-turbine results for the GTI relative to the ERS. As described, the presence of erratic data during the low wind-resource seasons of the 2003–2004 period led to the expectation of artificially elevated values for the GTI. At the ERS, the annual potential outputs for the 1994–2004 timeframe were 12.3 and 10.6 MWh, for the J&M and PL, respectively. The results for this site during the 2003–2004 period were 4.4% and 5.8% higher for the respective models, at 12.8

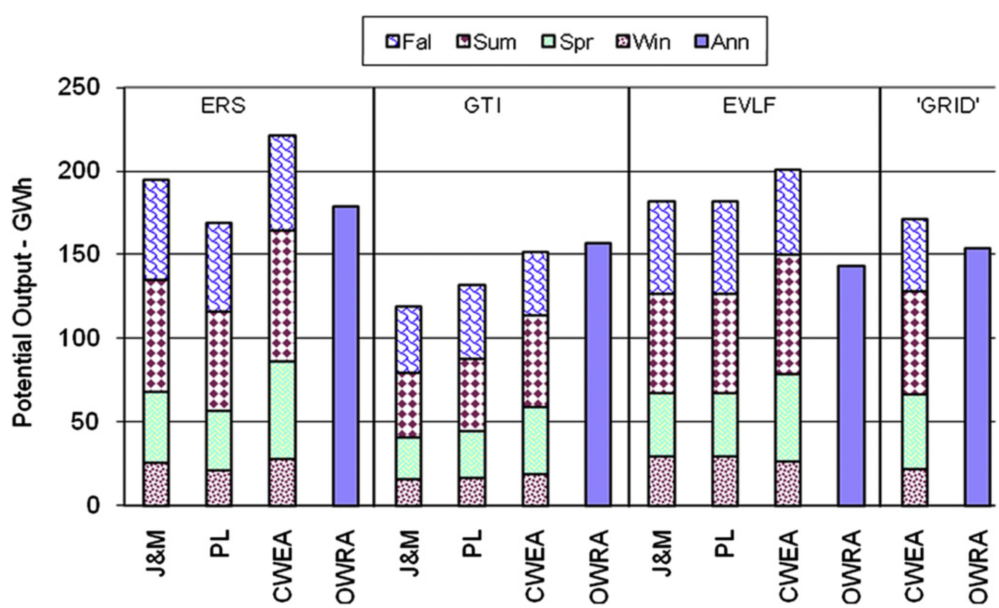

Fig. 8. Seasonal and annual production potential for an idealized community-scale, multi-turbine array of Bergey Excel-S wind turbines [1] at 30 m above ground with the longest period available for the J&M and PL.

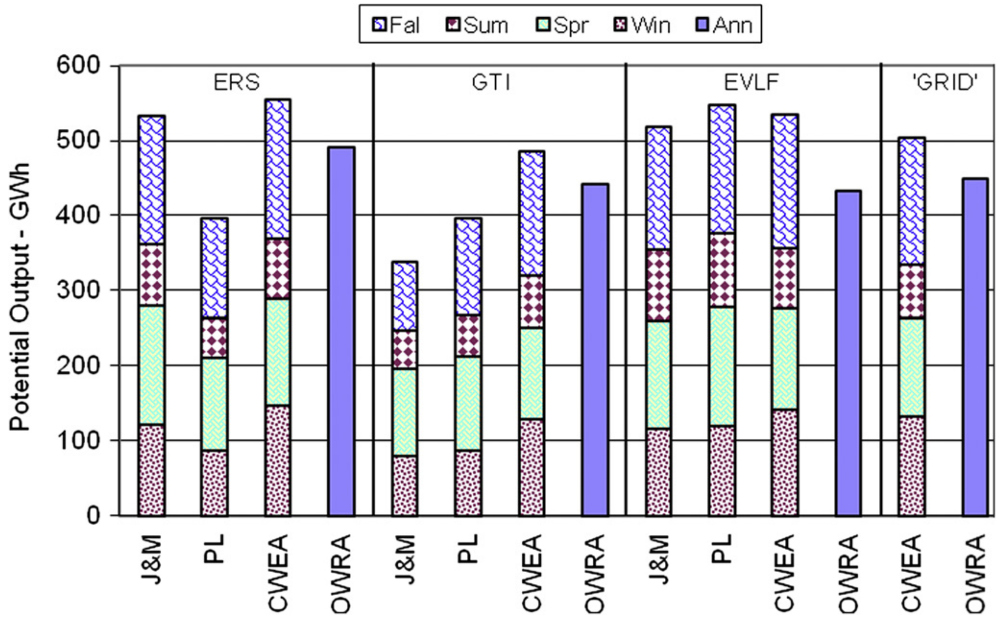

Fig. 9. Seasonal and annual production potential for an idealized community-scale, multi-turbine array of Vestas V82 wind turbines [25] at 80 m above ground with the longest period available for the J&M and PL.

and 11.2 MWh. A similar analysis for the GTI revealed relative increases of 8.9% and 9.4% during this period with the respective models. Assuming that the relative increases found for the ERS during this period were applicable to the GTI, the actual values for the GTI could have been closer to 7.9 and 8.9 MWh for the respective models. However, difficulties arise in resolving whether or not it is appropriate to use the PL for this estimate due to the use of different power law coefficients (PL, α) for the ERS and GTI sites. The coefficients utilized for the J&M are relatively similar for the two sites when compared to the coefficients for the PL. In addition, the quality of the results for the GTI during the 1994–2004 period could be scrutinized due to the proportion of valid data.

The use of data from two observation heights for the EVLF allowed for flexibility with the application of the models and led to four different results for the 2003–2004 period. A numerical average of the output results at 30 m for the 1-h EVLF data yielded an annual potential of 11.4 MWh with a standard deviation of 0.19 MWh. Similar analysis with the 10-min EVLF data yielded an annual average of 11.6 MWh with a standard deviation of 0.23 MWh. The potential output obtained with the observation data at 30 m (MMLM) for the J&M and PL was 10.2% less and 2.4% more than that of the ERS, for the respective models. The modeling of the 20 m EVLF data also yielded mixed results when compared with those of the ERS. The J&M provided electricity-production potentials that were 13.0% less, while those of the PL were 3.2% and 1.2% more for the assumed and calculated power coefficients, respectively.

The use of raw wind-speed data allowed for the direct estimation of the single-turbine production potential by applying the data to a cubic-regression model (CR) of the Bergey Excel-S power curve. Table 4 displays the results obtained via CR along with a comparison of those obtained via WPD parameters (i.e. Table 1 for the ERS and GTI; Table 2 for the EVLF). Here, a negative value indicates a CR production estimate that is less than that of the identified method (MMLM, J&M, or PL). This represents an apparent over-estimation by a method when compared with the potential output obtained from the direct application of wind-speed data via CR. The results show that the CR yielded both over- and under-estimations relative to the J&M and PL. The deviation ranged from 13.6% less to 9.4% more for the J&M and from 4.5% less to 1.2% more for the PL. The output potentials obtained with the CR are most consistent with those obtained with the PL. This is likely due to the reliance of CR on wind-speed data modified with the PL. A slight over-estimate (−1.8%) occurred with the use of the WPD on EVLF observation-height data in the absence of the PL or J&M (MMLM only).

The final part of this assessment utilized wind atlas data to estimate the potential output from a community-scale wind farm. Fig. 8 illustrates the production potential for an array of Bergey Excel-S turbines at 30 m above ground, while Fig. 9 reflects that with Vestas V82 turbines at 80 m. These figures include output potential obtained for the longest evaluated period of the individual sites as applied to the number of turbines in the idealized, community-scale array. This allows for a graphic comparison of the site production estimates with the values obtained from the wind atlases on the basis of the idealized arrays. As shown, the results for the models and wind atlases generally agree for the observation sites, with those for the ERS generally displaying the greatest potential. The results for potential electricity-production output indicated substantial seasonal variation. The values obtained for the winter season more than doubled those of the summer, each representing the high and low of the annual cycle, respectively. This trend matches that of Li and Li who observed that the monthly wind-speed average of February nearly doubles that of August [34].

Table 5 summarizes the potential output obtained from the idealized community-scale arrays and also provides a reference of energy and electricity use for the city of Guelph in 2005 [17]. The first part of this table provides the specifications for two versions of the idealized wind farms (Bergey versus Vestas at their corresponding operating height). As stated, our idealized array ignores placement issues (geographic features, building, etc.), and relies on a turbine footprint derived from the rotor diameter. This strategy produced total swept areas for the respective arrays of 17 697 Bergey Excel-S and 128 Vestas V82 wind turbines that differed by less than 1.0%. The second section of this table summarizes the annual potential for the sites in Guelph for the longest period evaluated as applied to our idealized array. Overall, the community-scale results generally agree, however we observed some spatial variation with those obtained for the individual grid points with the

Table 5
Annual community-scale, multi-turbine production potential at nominal hub heights.

Manufacturer and model	Bergey Excel-S	Vestas V82
Rated power output	10 kW	1.65 MW
Rotor diameter (m)	7	82
Hub height (m)	30	80
Land area per turbine (km^2)	0.00490	0.672
Number of turbines	17 697	128
Annual potential electricity output (GWh)[a]		
GTI – J&M	120	370
GTI – PL	134	401
GTI – CWEA	155	487
GTI – OWRA	157	442
EVLF – J&M	183	534
EVLF – PL	186	555
EVLF – CWEA	205	537
EVLF – OWRA	143	432
Guelph grid – CWEA	174	502
Range (min/max)	(141/233)	(466/560)
Guelph grid – OWRA	141	434
Range (min/max)	(106/187)	(368/514)
Demand (GWh) & relative potential for Guelph, 2005		
Total energy	6034	
GTI – J&M and PL	2.2%	6.6%
GTI – CWEA and OWRA	2.6%	7.7%
EVLF – J&M and PL	3.1%	9.2%
EVLF – CWEA and OWRA	2.9%	8.0%
Guelph grid – CWEA and OWRA	2.6%	7.8%
Electricity	1630	
GTI – J&M and PL	8.2%	24.6%
GTI – CWEA and OWRA	9.6%	28.5%
EVLF – J&M and PL	11.4%	34.0%
EVLF – CWEA and OWRA	10.7%	29.7%
Guelph grid – CWEA and OWRA	9.7%	28.7%

[a] 10% Power reduction for inter-turbine (downwind) losses.

respective wind atlases. The final section of Table 5 provides a comparison of production potential with the energy and electricity demand in Guelph for 2005. The results obtained with the 35-point grid show that the potential may exist for electricity production equivalent to 7.8% and 29% of the total energy and electricity use for Guelph in 2005, respectively, with 128 Vestas V82 turbines. The use of this strategy with Bergey Excel-S turbines could produce 2.6% and 9.7% of the total energy and electricity, respectively. These values indicate the potential that local wind-energy use could significantly contribute to the renewable-energy portfolio of Guelph. They also indicate the range of possibility for an array within the city limits of Guelph as one would likely consist of a mix of such turbines.

There is an evolving body of regulation and studies that relate to the size and proximity of wind turbines to occupied buildings that we excluded from this study. Concerned citizens continue to raise questions regarding the effect of large-scale wind turbines on human health. Dr. Nina Pierpont coined the phrase "Wind Turbine Syndrome" [35] for the impact of low-frequency vibrations that may result under certain conditions [36]. Wolsink [37] documented the known level of "NIMBYism" (i.e. Not In My Back Yard) that exists for this particular technology. He specifically discussed the concerns typically raised, formulates the potential for resistance to wind turbine siting, and alluded to the fact that these issues could affect the economics of installation. Other issues that may require assessment for site selection and evaluation include ice shedding and solar flicker. That said, this technology continues to gain acceptance. Often, it is a matter of whether or not society chooses to accept the risks (known and unknown) associated with the use of a specific technology.

5. Conclusions

1) Guelph may have the potential to obtain up to 7.8% and 29% of the 2005 total energy and electricity requirements, respectively, from a community wind turbine array.
2) The assessment of two turbines at separate hub heights for an ideal, city-wide array revealed the capacity for a 3-fold difference in potential output of electricity for Guelph.
3) The data sources examined in this study provided reasonably similar results for the sites of interest and with respect to the city-wide potential in Guelph.
4) Seasonal variation occurred in the wind-energy potential for Guelph, with the electricity-production potential of the 3-month winter period more than doubling that of the summer.
5) The deviation in the potential output due to the use of 10-min and 1-h sampling periods was inconsequential for the data evaluated.
6) The direct application of wind-speed data to a CR model of a turbine power curve yielded results that were consistent with those obtained with PL-WPD in 1 m/s bins.

Acknowledgements

The authors gratefully acknowledge the financial support of the NSERC (Canada) Chairs in Environmental Design Engineering Program. The authors thank Dean Wyman of the city of Guelph for providing the wind data taken at the Eastview Landfill site, as well as Martin K. Ince of M. K. Ince and Associates Ltd. who assessed the EVLF site and alerted the authors to the existence of this study. The authors also thank the staff of the Data Resource Centre at the University of Guelph for their assistance, and especially that of Teresa Lewitzky.

The authors have no specific interests in the manufacturers or products utilized in this study. The completion of this body of work has proceeded without their knowledge, consent, support, or influence.

References

[1] St. Denis G, Parker P. Community energy planning in Canada: the role of renewable energy. Renew Sust Energy Rev 2009;13(8):2088–95.
[2] EnEffect, Municipal energy planning: guide for municipal decision makers and experts. Available from: www.energie-cities.org; 2010 [accessed 10.09.10].
[3] Natural Resources Canada, community energy planning guide. Available from: www.smartgrowth.ca/research/cep/cep-sgcn.pdf; 2007 [accessed 10.09.10].
[4] Community Energy Association [British Columbia]. A tool kit for community energy planning in BC. Available from: http://www.communityenergy.bc.ca/community-energy-planning-toolkit-rev-2006; 2006 [accessed 10.09.10], 108 p.
[5] Canadian Urban Institute. Energy mapping study (for Calgary, Alberta, Canada). Available from: www.canurb.com; December 2008 [accessed 10.09.10], 90 p.
[6] Beatley T. Envisioning solar cities: urban futures powered by sustainable energy. J Urban Technol 2009;14(2):31–46.
[7] Cherry J. The windy city: harnessing power in the neighborhood landscape. Thesis, The Massachusetts Institute of Technology, Cambridge, MA; June, 2008.
[8] Toke D. Community wind power in Europe and in the UK. Wind Eng 2005;29 (3):301–8.
[9] Bolinger MA. Making European-style community wind power development work in the US. Renew Sust Energy Rev 2005;9(6):556–75.
[10] Elkinton MR, Rogers AL, McGowan JG. An investigation of wind-shear models and experimental data trends for different terrains. Wind Eng 2006;30(4):341–50.
[11] Eidsvik KJ. A system for wind power estimation in mountainous terrain. Prediction of Askervein hill data. Wind Energy 2005;8(2):237–49.
[12] Neff DE, Meroney RN. Wind tunnel modeling of hill and vegetation influence on wind power availability. J Wind Eng Ind Aerodyn 1998;74–76:335–43.
[13] Troen I, Petersen EL. European wind atlas. Roskilde, Denmark: Risø National Laboratory. Available from: http://www.windatlas.dk/europe/Index.htm; 1989 [accessed 10.09.10].

[14] Yu W, Benoit R, Girard C, Glazer A, Lemarquis D, Salmon J, et al. Wind energy simulation toolkit (WEST): a wind mapping system for use by the wind-energy industry. Wind Eng 2006;30(1):15–33.
[15] Statistics Canada. Population and dwelling counts, for census metropolitan areas and census agglomerations, 2006 and 2001 censuses – 100% data. Available from: http://www12.statcan.ca/english/census06/data/popdwell/Table.cfm?T=303&CMA=550&S=0&O=A&RPP=25; 5 November 2008 [accessed 26.02.10].
[16] C.N. Watson and Associates Ltd.. City of Guelph household and population projections 2001–2027 – final report; 29 April 2003.
[17] Garforth International LLC. City of Guelph community energy plan. Available from: http://guelph.ca/living.cfm?smocid=2127; 16 March 2007 [accessed 23.03.09].
[18] McIntyre JH, Lubitz WD, Stiver WH. Wind energy resource assessment using wind atlas and meteorological data for the city of Guelph, Canada. In: 7th World Wind Energy Conference 2008. Kingston, ON: Community Power. Available from: http://www.ontario-sea.org/Storage/26/1810_Wind_Energy_Resource_Assessment_and_Siting_Analysis_Using_Wind_Atlas_adn_Meteorological_Data_for_the_City_of_Guelph,_Canada.pdf; 2008 [accessed 10.09.10].
[19] University of Guelph, Department of Land Resource Science. Weather records for Elora Research Station & Guelph Turfgrass Institute [GTI monthly data files and ERS monthly data]. Available from: http://www.uoguelph.ca/~wxrecord/; 2007 [accessed 21.01.08; additional data provided via personal communication].
[20] Wyman Dean. The city of Guelph Eastview landfill wind data. Personal communication; December, 2008.
[21] Environment Canada. Canadian wind energy atlas. Available from: http://www.windatlas.ca/en/index.php; 2008 [accessed 17.02.10].
[22] Ontario Ministry of Natural Resources. Wind resource atlas. Available from: http://www.ontariowindatlas.ca/en/welcome.html; 2006 [accessed 17.02.10].
[23] Ontario Ministry of Natural Resources & Hélimax – Jean Pauquin and Norme Raine, respectively. Resolution of wind resource atlas. Personal communication; April 2008.
[24] Bergey Windpower Co.. Technical materials–WindCAD performance models–10 kW Excel-S (Grid – Intertie; 2004, version 3 blades). Available from: http://www.bergey.com/Technical/ExcelS.xls; 2004 [accessed 07.03.08].
[25] Vestas, V-82–1.65 MW, creating more from less. Available from: http://www.vestas.com/Admin/Public/Download.aspx?file=/Files/Filer/EN/Brochures/ProductBrochureV821_65_UK.pdf; 2008 [accessed 17.03.08].
[26] Manwell JF, McGowan JG, Rogers AL. Wind energy explained: theory, design and application. West Sussex, England: John Wiley & Sons Ltd; 2002.
[27] Counihan J. Adiabatic atmospheric boundary layers: a review and analysis of data from the period 1880–1972. Atmos Environ 1975;9(10):871–905.
[28] Weibull W. A statistical distribution function of wide applicability. J Appl Mech 1951;18(3):293–7.
[29] Patel MR. Wind and solar power systems. New York: CRC Press; 1999.
[30] Lun IYF, Lam JC. A study of Weibull parameters using long-term wind observations. Renew Energy 2000;20(2):145–53.
[31] Seguro JV, Lambert TW. Modern estimation of the parameters of the Weibull wind speed distribution for wind energy analysis. J Wind Eng Ind Aerodyn 2000;85(1):75–84.
[32] International Electrotechnical Commission. Wind turbines – part 12–1: power performance measurements of electricity producing wind turbines, IEC 61400-12 international standard; 2009.
[33] Justus CG, Mikhail A. Height variation of wind speed and wind distribution statistics. Geophys Res Lett 1976;3(5):261–4.
[34] Li M, Li X. Investigation of wind characteristics and assessment of wind energy potential for Waterloo region, Canada. Energy Convers Manage 2005;46(18–19). 3014–3013.
[35] Piermont N. Wind turbine syndrome – Nina Piermont's research. Available from: http://www.windturbinesyndrome.com/; 2009 [accessed 27.04.09].
[36] Todd NP, McAngus SM, RosengrenColebatch JG. Tuning and sensitivity of the human vestibular system to low-frequency vibration. Neurosci Lett 2008;444(1):36–41.
[37] Wolsink M. Wind power and the NIMBY-myth: institutional capacity and the limited significance of public support. Renew Energy 2000;21(1):49–64.